***Bull. Egypt. Soc. Physiol. Sci.*** *Vol. (44), Issue (3)*, 150-168

**Bull. of Egyp. Soc. Physiol. Sci.**

(Official Journal of Egyptian Society for Physiological Sciences)

**(pISSN: 1110-0842; eISSN: 2356-9514)**

# Ameliorative effect of resveratrol against type 2 diabetes in rats through triggering of autophagy and inhibition of mTOR pathway

Lina Abdelhady Mohammed[1], Ahmed Medhat Hegazy[2*], WalaaBayoumie El Gazzar[1], Noha Osama El-Shaer[3], Heba Bayoumi[4], Salwa A. Elgendy[5], Heba A. Elnoury[5], HendElsayed Nasr[1]

[1]Department of Medical Biochemistry and Molecular Biology, Faculty of Medicine, Benha University, Benha 13518, Egypt.
[2]Department of Forensic Medicine and Toxicology, Faculty of Veterinary Medicine, Benha University, Moshtohor, Toukh 13736, Qalyubia, Egypt.
[3]Department of Physiology, Faculty of Medicine, Benha University, Benha 13518, Egypt.
[4]Department of Histology and Cell Biology, Faculty of Medicine, Benha University, Benha 13518, Egypt.
[5]Deparment of Pharmacology, Faculty of Medicine, Benha University, Benha 13518, Egypt.

**Submit Date :** 26 March 2024
**Accept Date :** 14 April 2024

## Keywords

- autophagy,
- mTOR pathway
- oxidative stress
- resveratrol
- type 2 diabetes mellitus

## Abstract

**Background:**Type 2 diabetes mellitus (T2DM), which affects millions of individuals, has become a serious health problem.The mammalian target of rapamycin (mTOR) hyperactivation is a negatively involved autophagy that may in fact aid in theloss of β-cell function.Resveratrol (RSV) is a naturally occurring phytoalexin, mostly found incereals, fruits, and vegetables that have antioxidant effects. **Aim:**In the current work, Wistar rats exposed to high-fat diet (HFD) and streptozotocin (STZ)-induced T2DM were evaluated for resveratrol's protective effects on pancreatic functions, and mTOR-mediated autophagy. **Materials and Methods:**Four equal groups of forty male Wistar rats were created at random.Group 1 (G1) was maintained in typical control circumstances and given a balanced diet;G2, G3, and G4 were fed HFD for 10 weeks continuously; at the end of the 6$^{th}$ week injected I/P STZ as a single dose to induce T2DM. Three days after diabetic induction, G3 was received RSV daily for continuously 4 weeks. G4 was received RSV in addition to Chloroquine (CQ) as autophagy inhibitor. **Results:**The findings shown that RSV reduces the pancreatic dysfunctions brought on by HFD-STZ by inhibiting the mTOR pathway through decreasing the level of mTOR, Cas-3, and p62 and increasing the level of LC3.RSV activate autophagy and inhibit apoptotic-mediated cell death confirmed by transmission electron micrograph findings. **Conclusion:**RSV is thought to protect pancreatic cells by inhibiting the mTOR pathway, which regulates the transition between autophagy and apoptotic machinery in diabetic circumstances.

**Corresponding author: Ahmed Medhat Hegazy**: Department of Forensic Medicine and Toxicology, Faculty of Veterinary Medicine, Benha University, Moshtohor, Toukh 13736, Qalyubia, Egypt. E-mail: ahmed_medhat012@yahoo.com, ahmed.hegazy@fvtm.bu.edu.eg Mobile: +201005192110

**Introduction**

Hyperglycemia is a hallmark of diabetes mellitus (DM), which has been defined as a metabolic condition brought on by problems with insulin secretion. Type 2 diabetes mellitus (T2DM), which affects millions of individuals, has emerged as a severe health issue that lowers life expectancy and quality. The failure of the insulin producing β cells, which is at least partially brought on by an increase in cell apoptosis, is central to the pathophysiology of diabetes.The mechanisms that trigger apoptosis in the onset of diabetes are still poorly understood[1].

The process of autophagy is essential for preserving cellular homeostasis and aids in the survival of cells under stress.In the catabolic process known as autophagy (self-eating), proteins and whole cell organelles are engulfed by double-membrane vesicles called autophagosomes.Following delivery to lysosomes, the autophagosomes' contents are broken down and recycled as simple basic biomolecules back into the cytosol [2]. When nutrients are few, cells use autophagy to recycle fundamental biomolecules, scavenge damaged organelles and toxic proteins, and get rid of intracellular pathogens [3].

Kinases and multiprotein complexes control autophagy. The mTOR (mammalian target of rapamycin) route is a negatively implicated autophagy process, whereas the adenosine 5'-monophosphate (AMP)-activated protein kinase (AMPK) pathway is positively mediated. Previous research has connected the development of endoplasmic reticulum (ER) stress with mTOR1 hyperactivationresulting inthe loss of β-cell function [4].A number of diseases, particularly neurodegenerative disorders, cardiovascular diseases, and diabetes [5] have impaired autophagy as part of their pathophysiology.

Resveratrol (RSV), a naturally occurring phytoalexin, is mostly found in dry legumes, cereals, fruits, and vegetables.RSV has a range of biological and pharmacological properties, including those that are anti-inflammatory, anti-oxidant, and anti-obesity. Recently, it was discovered that RSV could prevent myocardial ischemia/reperfusion injury by raising the degree of autophagy[6].Zhang et al[7] showed that RSV can lessen hepatic fibrosis by targeting autophagy and apoptosis as potential treatment targets. Through its ability to induce autophagy, concurrent therapy with resveratrol resulted in a clear improvement of retinopathy[8].The current studies aimed to evaluate the potential protective benefits of RSV on the pancreatic functions of Wistar rats exposed to HFD and streptozotocin (STZ)-caused T2DM as well as the role of autophagy as a potential underlying mechanism.

**Material and methods**

**Ethical approval**

The current study was conducted in accordance with the Institutional Animal Ethics Committee's regulations, as well as Approval Protocol Number: BUFVTM 11-11-22 from Benha University in Egypt.

**Chemicals**

Streptozotocinpowder (STZ) (Cat#18883-66-4) was purchased from AldrichCompany, St. Louis, MO, USA. Resveratrol (RSV) (Cat# NC9382296) was purchased from Cayman Chemicals, MI, USA.Chloroquine (CQ) (hydroquine) was purchased from Mina pharm on the tenth of

Ramadan,for the pharmaceutical and chemical industries in Egypt.

**Composition of diets**

The National Research Council (NRC)[9]was used as the basis for the balanced diet composition (Table 1). According to Table (2), it comprised crude fat (5.08%), metabolizable energy (ME) (2769.97kcal/kg diet), and crude protein (18.07%). The NRC[9]served as the basis for the formulation of the HFD (Table 3). According to Table 2, it comprised crude fat (30.03%), ME (4103.18kcal/kg diet), and crude protein (18.02%).

**Table 1. Ingredients of the balanced diet.**

| Feed ingredients | Diet (%) |
|---|---|
| Yellow corn | 24.50 |
| Wheat grains | 23.00 |
| Soybean meal 46 | 12.80 |
| Wheat shorts | 12.00 |
| Wheat Bran | 9.15 |
| Skim milk powder | 5.00 |
| Fish meal 65 % CP | 5.00 |
| Molasses Cane | 3.50 |
| Vegetable oil | 2.50 |
| Di calcium phosphate | 1.25 |
| Lime stone | 0.50 |
| Sodium chloride | 0.50 |
| Vitamin& mineral premix1 | 0.30 |
| Total | 100.00 |

**Table 2. Chemical constituents of the balanced and high fat diet (HFD).**

| Item | Balanced diet | HFD |
|---|---|---|
| Metabolizable energy (kcal/kg diet) | 2769.97 | 4103.18 |
| Crude protein | 18.07 % | 18.02 % |
| Crude fat | 5.08 % | 30.03 % |

**Table 3. Ingredients of the high fat diet (HFD).**

| Feed ingredients | Diet (%) |
|---|---|
| Vegetable oil | 27.80 |
| Wheat Bran | 23.05 |
| Yellow corn | 12.70 |
| Wheat Feed Flour | 10.00 |
| Soybean meal 46 | 9.80 |
| Fish meal 65 % CP | 9.20 |
| Skim milk powder | 5.00 |
| Amin MAG | 1.30 |
| Sodium chloride | 0.50 |
| Vitamin and mineral premix 1 | 0.30 |
| Di calcium phosphate | 0.20 |
| DL-Methionine | 0.10 |
| Lime stone | 0.05 |
| Total | 100.00 |

**Experimental animals**

Four to five week old male adult Wistar rats (weighing 130 to 150 g) were purchased from the National Research Centre's Animal House in Dokky, Giza, Egypt. The rats were kept in tidy cages and were provided with clean food and water on demand. All rats were kept in standard conditions, including a room temperature of 23°C, a 12-hour light/dark cycle, and free access to food and water. Rats were destroyed using an incinerator when the study's sample collection was finished.

**Induction of diabetes mellitus**

For induction of T2DM, streptozotocin (STZ) and a high fat diet (HFD) were used. The rats fed on HFD for continuously 10th weeks. At the end of the 6th week of the experiment, rats wereinjected I/P STZ prepared in 0.01 M citrate buffer (pH 4.4)at a dose of 35 mg/kg b.wt.as a single dose to individual rat [10]. To prevent hypoglycemia, the rats sipped a 5% glucose solution throughout the night. By checking the blood glucose levels (after an overnight fast), T2DM was confirmed 72 hours later.Diabetes mellitus was defined as having a glucose level of 180 mg/dl or higher[11].

**Experimental design**

A total of 40 male Wistar rats were divided into four equal groups, each with ten animals. The initial group (G1) was kept as a healthy control and given a balanced diet. The second, third, and fourth groups were fed HFD for 10 weeks continuously, then at the end of the 6th week they were injected I/P STZ at a dose of 35 mg/kg b.wt.as a single dose to induce T2DM. Three days after diabetic induction,the third group (G3) was receivedRSV dissolved in ethanol by stomach tube at a dose of 5 mg/kg b.wt.daily for continuously 4 weeks[12]. The fourth group (G4) wasreceived RSV at the same dose and duration of G3 in addition to Chloroquine (CQ) as autophagy inhibitor. G4 was injected I/P CQ at a dose of 60 mg/kg b.wt. daily for continuously 4 weeks[13].The experimental rats were euthanized with isoflurane at the end of the study (10 weeks and 3 days) before being killed by decapitation.For measurements of the levels of glucose, insulin, oxidative markers, pancreatic protein markers, histopathological alterations, immunohistochemistry, and transmission electron micrograph (TEM) inspection, blood samples from the abdominal aorta and pancreatic tissues were obtained.

**Preparation of pancreatic tissue homogenate**

According toEl-Shaer et al[14], pancreatic tissue homogenates were prepared. The oxidative indicators [lipid peroxidation by-products (MDA), superoxide dismutase activity (SOD), and quantity of reduced glutathione (GSH)] and total protein were measured in the collected supernatant.

**Assay methods**

According to Trinder[15],the fasting serum glucose level was measured. The method ofGroen et al[16] was used to estimate the fasting serum insulin level.

**Lipid profile**

According to Cox et al[17], the serum triglycerides (TG), total cholesterol (TC), and high density lipoprotein cholesterol (HDL-C) were measured. The method ofMartin et al[18]was used to determine the serum low density lipoprotein cholesterol (LDL-C).

**Oxidative markers in pancreatic tissue homogenate**

According toGarcia et al[19], the MDA (as lipid peroxidation by-products) in pancreatic tissue homogenate was measured. SOD activity was measured in accordance with Flohe[20]. According toEllman[21], the reduced glutathione (GSH) content was determined. The method ofLowry[22] was used to determine the homogenate's total protein content.

**Protein markers in pancreatic tissue homogenate**

We used the Bio-Rad Inc. ReadyPrepTM protein extraction kit (Catalogue #163-2086) for pancreatic tissue proteins extraction. Using the

Bradford Protein Assay Kit (SK3041) from Bio Basic INC (Markham, Ontario, L3R 8T4 Canada), protein concentrations were assessed. The loading quantity of protein samples were 20µg. The extracts were separated by Sodium Dodecyl Sulfate PolyAcrylamide Gel Electrophoresis (SDS-PAGE)(12%), and then transferred to polyvinyllidene fluoride (PVDF) membrane (7min at 25V). The membrane was treated with a number of primary antibodies after blocking for an hour at room temperature with tris-buffered saline with Tween 20 (TBST) buffer and 3% bovine serum albumin (BSA).Then the primary antibodieswere treated at $4^{o}$Covernight as anti-LC3 (catalog no. 667819, Merck,Germany), anti-p62 (catalog no. sc-48389, SANTA CRUZ BIOTECHNOLOGY, INC. Europe), anti-phospho-mTOR (catalog no. 2971, Cell Signaling Technology, USA), anti-caspase-3 (catalog no. 100-56113, Novus Biological Inc, Littleton, CO, USA)and anti-β actin (housekeeping protein).The blot was rinsing with TBST 3-5 times for 5 minutes. The target protein was incubated in the HRP-conjugated secondary antibody solution (Goat anti-rabbit IgG-HRP-1mg Goat mab- Novus Biologicals) for 1 hour at room temperature. The blot was then washed 3-5 times for 5 min with TBST. The blot was covered with the chemiluminescent substrate (Catalogue no. 170-5060, ClarityTM Western ECL substrate Bio-Rad). A CCD camera-based imager was used to record the chemiluminescent signals. By protein normalization on the ChemiDoc MP imager, band intensity of the target proteins was read against the control sample β-actin (housekeeping protein).

**Histopathological examination**

All groups had pancreatic samples collected right away, which were then fixed for 24 hours in 10% buffered neutral formalin. Following convenient fixing, the samples were cleaned in xylol, embedded in paraffin, dehydrated in various grades of ethyl alcohol, blocked, and sectioned into 5µm thick sections. Followed by hematoxylin and eosin staining and microscopic examination[23].

**Immunohistochemical study**

The manufacturer's instructions were followed for doing the immunohistochemical staining. Avidin-biotin peroxidase was employed. On coated slides, paraffin slices were mounted. In order to inhibit endogenous peroxidase activity, they were deparaffinized in xylene, rehydrated in descending grades of alcohol, and then submerged in 0.3% hydrogen peroxide for 30min. The slices were treated with 1:100 diluted monoclonal mouse antibodies to the human insulin protein for 1 hour.The secondary antibody (biotinylated goat anti-mouse IgG, DAKO LSAB 2 Kit; Dako, Glostrup, Denmark) was incubated on the slides for 1 hour at room temperature before they were once again rinsed in PBS. 0.05% diaminobenzidine was used to see the immunoreactivity. Hematoxylin was used as a counterstain on pancreatic sections for 4min. PBS was used in place of the main antibody as a negative control. Using Image J analysis, the area stained in brown-yellow was determined to be a positive area after four high-power fields were randomly chosen from each section [24].

**Computer Assisted digital image analysis (Digital morphometric study)**

Four random fields from each of the two prepared slides for each rat were examined. With a 0.5 X

photo adaptor attached to an Olympus microscope and a 40 X objective, slides were photographed and saved as TIFF files. The results were saved to an Excel sheet and expressed as integrated density. The result photos were analyzed on an Intel® Core I7® based computer using the Video Test Morphology® programme (Russia) with a special built-in routine for stain quantification.

**Ultrastructure of the pancreas**

**Transmission electron micrograph (TEM) processing**

Using a 1 $mm^3$ dissection technique, pancreatic specimens were preserved for 60min in 2% glutaraldehyde buffered with sodium cacodylate at pH 7.2. The samples were then soaked for two hours in 0.1M phosphate buffer solution (PBS), pH 7.4, at $4^oC$, followed by three PBS washes lasting ten minutes each. The samples were then post-fixed for 30min in 1% osmic acid, followed by three PBS washes lasting 10min each. Samples were dehydrated for 30min using an ascending series of ethyl alcohol concentrations (30, 50, 70, 90%, and absolute alcohol).Following an hour of acetone infiltration, samples were embedded in Araldite 502 resin. Utilizing an LEICA Ultracut (UCT ultra-microtome) to cut the plastic moulds, they were then dyed with 1% toluidine blue. After studying semi-thin sections, ultra-thin sections (50–60 nm thick) were cut, stained with uranyl acetate, followed by lead citrate, analyzed, and captured on camera using a JEOL–JEM–100 SX electron microscope, Japan [25].

**Statistical analysis**

For statistical analysis, SPSS for Windows (Version 20.0; SPSS Inc., Chicago, Illinois) was employed. In order to assess the significance of differences between more than two groups, one-way analysis of variance (ANOVA) was utilized. If it showed a significant difference, Duncan's post hoc test was used to analyze the differences within each group. Results are given as the mean±standard deviation of the mean. A *p* value of 0.05 or less was regarded as significant.

**Results**

No mortalities between the various treatment groups were noted during the experimental period.

**Serum glucose and insulin**

Table 4 displays the mean and standard deviation upwards of the various groups' serum glucose and insulin levels. In both diabetic rats (G2)and diabetic rats treated with RSV and CQ (G4), the fasting serum glucose level increased noticeably compared to normal control group after 10 weeks of the experiment. However, following 10 weeks of experiment, diabetic rats co-treated with RSV (G3) had significantly lower fasting serum glucose levels than the diabetic group. Insulin level also noticeably decreased in the diabetic group (G2)and diabetic group treated with RSV and CQ (G4) than the control group. However, after 10 weeks of experiment, diabetic rats treated with RSV (G3) displayed considerable increases in insulin level.

**Changes in the lipid profile**

Table 5 shows the lipid profile mean and standard deviation values for the various groups. The level of TG, TC, LDL were markedly increased in both the diabetic rats (G2) and diabetic rats treated with bothRSV and CQ (G4) than normal control group (G1). While after 10 weeks of the investigation, co-treatment of the diabetic group with RSV revealed significant reductions in TG, TC, and LDL levels as compared to the diabetic group.On the other hand, there were no significant differencesin the values of HDL-C between the

diabetic group (G2), diabetic grouptreated with RSV (G3), and diabetic grouptreated with both RSV and CQ(G4) after 10 weeks of the experiment.

**Changes in the pancreatic oxidative markers**

Table 6 shows the mean and standard deviation of the individual groups' oxidative markers. Both diabetic rats (G2) and diabetic rats treated with RSV and CQ (G4) had significantly higher levels of MDA in the pancreatic tissue than the healthy control group. While treatment of the diabetic group with RSV(G3) showed significant decreases in MDA level when compared with the diabetic group after 10 weeks of the experiment. Likewise, the values of GSH and SOD in the pancreatic tissue of both the diabetic rats and diabetic rats treated with RSV and CQ markedly decreased than the normalcontrol group. However, treatment of the diabetic rats with RSVresulted in a considerable rise in the GSH content leveland SOD activity when compared with the diabetic group after 10 weeks of the experiment.

**Table 4.Effect of resveratrol against high fat diet (HFD) and streptozotocin (STZ) on serum glucose level and insulin in various gatherings of the experiment after 10 weeks of treatment (mean±standard deviation), (n=10).**

| Groups | G1 | G2 | G3 | G4 |
|---|---|---|---|---|
| Glucose (mg/dl) | 85.878±3.320$^{c}$ | 201.211±6.286$^{a}$ | 104.593±3.256$^{b}$ | 194.841±7.382$^{a}$ |
| Insulin (µIU/ml) | 24.885±1.627$^{a}$ | 2.744±1.214$^{c}$ | 19.471±2.870$^{b}$ | 4.582±1.053$^{c}$ |

Means with different superscripts in the same row are significantly different at p<0.05**.**
G1: rats were fed a balanced diet and serve as a normal control group.
G2: rats were fed HFD and injected STZ.
G3: rats were fed HFD and injected STZ then treated with RSV.
G4: rats were fed HFD and injected STZ then treated with RSV and Chloroquine.

**Table 5. Effect of resveratrol against high fat diet (HFD) and streptozotocin (STZ) on lipid profile in various gatherings of the experiment after 10 weeks of treatment (mean±standard deviation), (n=10).**

| Groups | G1 | G2 | G3 | G4 |
|---|---|---|---|---|
| Serum TG (mg/dl) | 89.959±5.749$^{d}$ | 231.537±2.109$^{a}$ | 123.427±9.073$^{c}$ | 191.047±5.060$^{b}$ |
| Serum TC (mg/dl) | 129.456±4.650$^{d}$ | 278.660±6.651$^{a}$ | 163.322±4.291$^{c}$ | 191.157±2.354$^{b}$ |
| Serum HDL-C (mg/dl) | 76.107±2.768$^{a}$ | 38.976±2.854$^{b}$ | 41.154±1.163$^{b}$ | 38.766±3.617$^{b}$ |
| Serum LDL-C (mg/dl) | 53.773±1.550$^{d}$ | 107.081±6.803$^{a}$ | 67.684±2.646$^{c}$ | 86.321±1.521$^{b}$ |

Means with different superscripts in the same row are significantly different at p<0.05**.**
G1: rats were fed a balanced diet and serve as a normal control group.
G2: rats were fed HFD and injected STZ.
G3: rats were fed HFD and injected STZ then treated with RSV.
G4: rats were fed HFD and injected STZ then treated with RSV and Chloroquine.

**Table 6.Effect of resveratrol against high fat diet (HFD) and streptozotocin (STZ) on oxidative markers in the pancreatic tissue homogenates of various gatherings of the experiment after 10 weeks of treatment (mean±standard deviation), (n=10).**

| Groups | G1 | G2 | G3 | G4 |
|---|---|---|---|---|
| MDA (nmol/mg protein) | 11.164±1.191$^{c}$ | 41.934±2.085$^{a}$ | 19.469±2.643$^{b}$ | 39.598±0.695$^{a}$ |
| SOD (U/mg protein) | 9.239±0.752$^{a}$ | 1.445±0.482$^{c}$ | 7.232±0.985$^{b}$ | 1.733±0.388$^{c}$ |
| GSH (µmol/mg protein) | 28.335±3.023$^{a}$ | 10.835±0.869$^{c}$ | 21.908±1.586$^{b}$ | 12.178±1.589$^{c}$ |

Means with different superscripts in the same row are significantly different at p<0.05**.**
G1: rats were fed a balanced diet and serve as a normal control group.
G2: rats were fed HFD and injected STZ.
G3: rats were fed HFD and injected STZ then treated with RSV.
G4: rats were fed HFD and injected STZ then treated with RSV and Chloroquine.

**Changes in pancreatic protein markers**

As displayed in Figure 1, the average relative density of pancreaticmTOR, Cas-3, LC3, and P62 normalized to β-actin in the diabetic, diabetic-resveratrol treated and diabetic-resveratrol-chloroquine treated groups than normal control group after 10 weeks of treatment. Comparing the diabetes group (G2) to the healthy control group, there were noticeably higher levels of mTOR, Cas-3, and P62 as well as a substantial drop in LC3 protein markers in pancreatic tissue. After 10 weeks of the experiment, the diabetic group that had received resveratrol treatment (G3) had significantly lower levels of mTOR, Cas-3, and P62 as well as significantly higher levels of LC3 compared to the control group (G2). Also, diabetic group treated with both RSV and CQ (G4) showed significant increase in Cas-3 and P62 as well as no significant differences in mTOR and LC3 compared to diabetic group treated with RSV (G3).

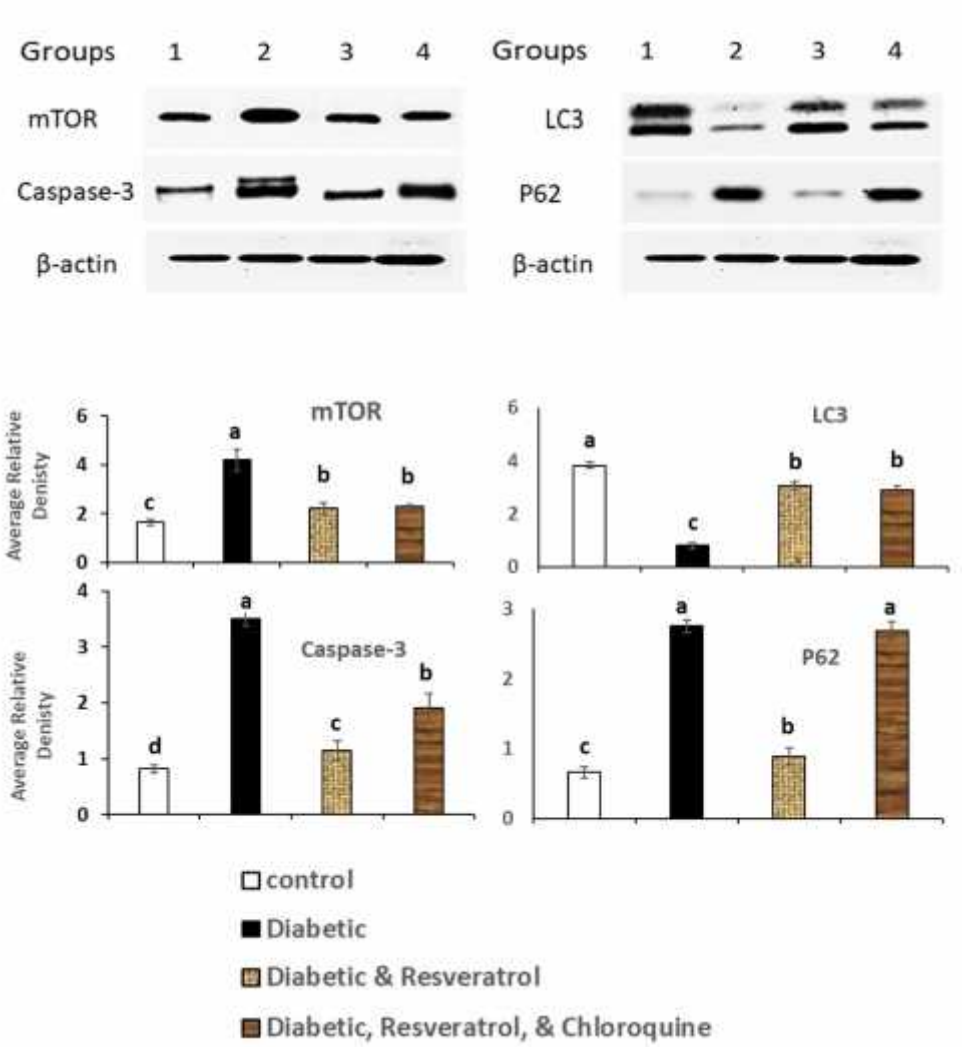


**Fig. 1** Western blotting with densitometric analysis of the autophagy and apoptotic-related proteins mTOR, Cas-3, LC3, and P62 in pancreatic tissue (n=10).

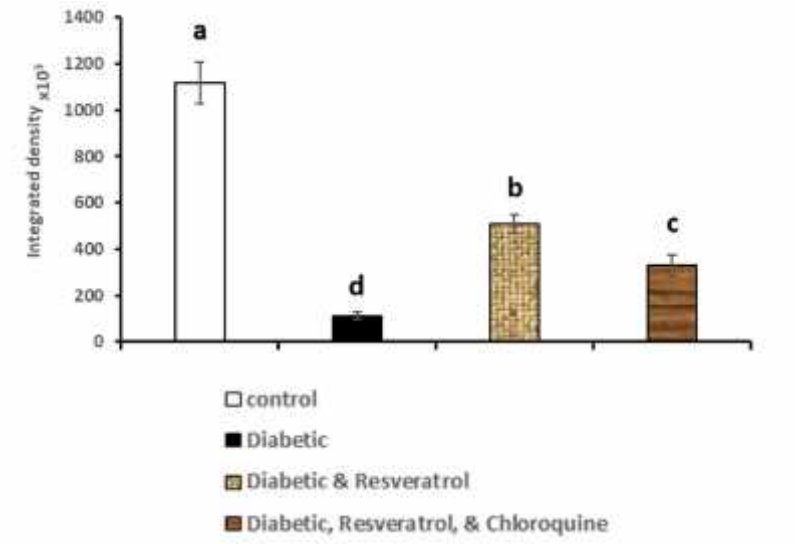


**Fig. 2**Integrated density of insulin immunohistochemical staining sections of pancreatic islets of various gatherings of the experiment after 10 weeks of treatment (n=10).

**Histopathological assessment of pancreatic tissue**

Pancreatic sections examined observed that diabetic rats exposed to HFD with STZ (G2) showed ill-defined areas of endocrine pancreas with marked histological distortion. The exocrine pancreas (Ex) showed multiple congested blood vessels (bent arrow)(Figure 3-b). Higher magnification of the black-boxedareashowed islet of Langerhans thatappeared shrunken with irregular outlines. The islet cells apparently decreased in number with pyknotic nuclei (arrows) and congested capillaries in between (c). There were multiple congested blood vessels (bent arrows) between the exocrine acini (Figure 4-b). Also diabetic rats exposed to both RSV and CQ (G4) showed marked histological alterations in the structure of endocrine pancreas (En) (Figure 3-d). Higher magnification of the black-boxed area showed distorted islet of Langerhans with irregular outlines. Some apoptotic cells (arrows) appeared with dense cytoplasm and pkknotic nuclei. Some other cells showed vacuolations (v). The CT septa infiltrated with inflammatory cells (angled arrow)(Figure 4-d). While diabetic rats treated with RSV (G3) showed the nearly normal appearance of the pancreas(Figure 3-c).Higher magnification of the black-boxed area showed nearly normal well defined islet of Langerhans (IL). The islet showed β-cells located in the center with vesicular nucleus (arrow), some cells still showing vacuolated cytoplasm (v). (Figure 4-c). The pancreatic tissues of control group (G1) appeared to be normal (Figure 3-a) and (Figure 4-a).

**Immunohistochemicalassessment of pancreatic tissue**

Insulin immunohistochemical staining sections of pancreatic islets observed that diabetic rats exposed to HFD with STZ(G2) and diabetic rats exposed to both RSV and CQ(G4) showed apparent marked reduction in the immunoreactivity of insulin in β-cells, only few cells showing brown immunostaining (arrow) (Figure 5-b) and (Figure 5-d). While diabetic rats treated with RSV showed an apparent increase in the immunoreactivity of insulin β-cells (arrow) mostly similar to the control group (Figure 5-c).

Insulin immunohistochemical staining sections of pancreatic islets of control rats showed typical islet strong positive immunoreactivity of insulin appeared as deep brown color (arrow) in β-cells which occupy most of the islet and surrounded by pale mantle zone with negatively stained cells (angled arrow) (Figure 5-a) (Figure 2).

**Transmission electron micrograph of the pancreatic tissue**

**Ultrastructure changes on pancreatic tissue**

Transmission electron micrograph of the pancreatic tissue on the control rats showed typical β-cell architecture with euchromatic nuclei (N), a well-developed Golgi complex (G), mitochondria (m), an electron-dense insulin granules surrounded by lucent halos (arrow) and an autophagosome (square). The cell junctions (angled arrow) between β-cells and blood capillary in the islet (C) can be seen (Figure 6-a). Diabetic rats exposed to HFD and STZ (G2) showed degenerated β-cell with nuclear shrinkage (N), electron dense heterochromatin (h), cytoplasmic rarefaction with marked vacuolation (v), degenerated mitochondria (m), empty insulin granules (arrows) and cystic dilatation of the rough endoplasmic reticulum (rER) (curved-arrow). There were large areas of lost granules (a strike) (Figure 6-b). Also diabetic rats treated with both RSV and CQ(G4) showed degenerated β-cell with empty insulin granules (arrows) and cystic dilatation rER (curved-arrow). The adjacent β-cell showed nearly normal insulin granules (rectangle) (Figure 6-d). While diabetic rats treated with RSV (G3) showed nearly normal β-cell except for slight chromatin condensation in the nucleus (N). The cytoplasm showed nearly normal insulin granules (arrows) and some autophagosomes (squares) (Figure 6-c).

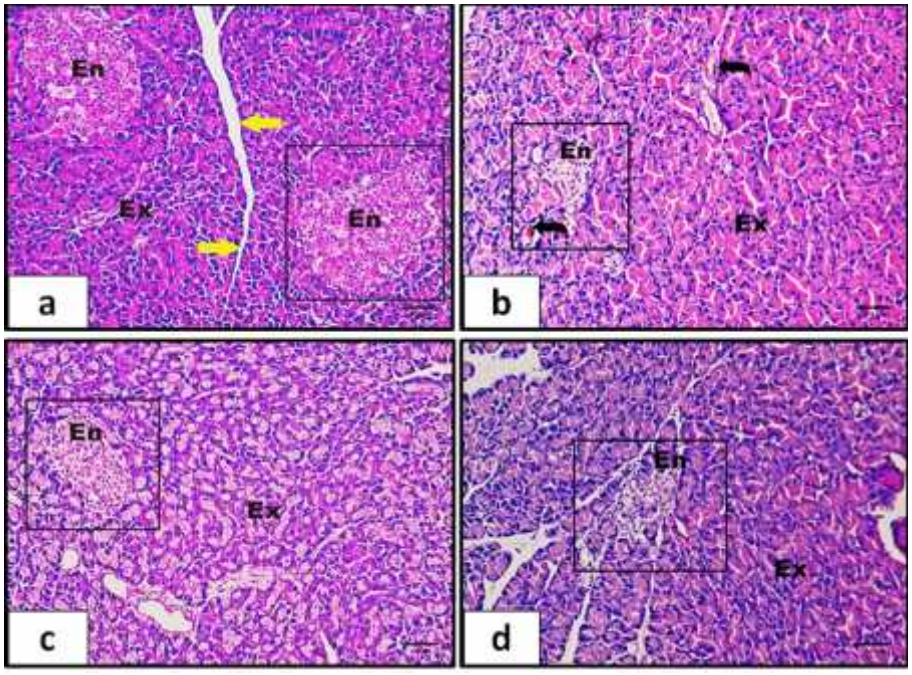


**Fig. 3** Photomicrograph from pancreas of experimental rats. (a) Normal control rat (G1), the pancreas showing a normal histological structure of both exocrine (Ex) and endocrine (En) pancreas with no abnormalities. (b) Diabetic rats (G2) induced by HFD with STZ. The pancreas showing ill-defined areas of endocrine pancreas (En) with marked histological distortion. The exocrine pancreas (Ex) showed multiple congested blood vessels (bent arrow). (c) Diabetic rats (G3)treated with resveratrol (RSV)showing the nearly normal appearance of the pancreas. (d) Diabetic rat exposed to both RSV and chloroquine (CQ) (G4), showing marked histological alterations in the structure of endocrine pancreas (En).(H&E, ×100)(Scale bar represents 40μm).

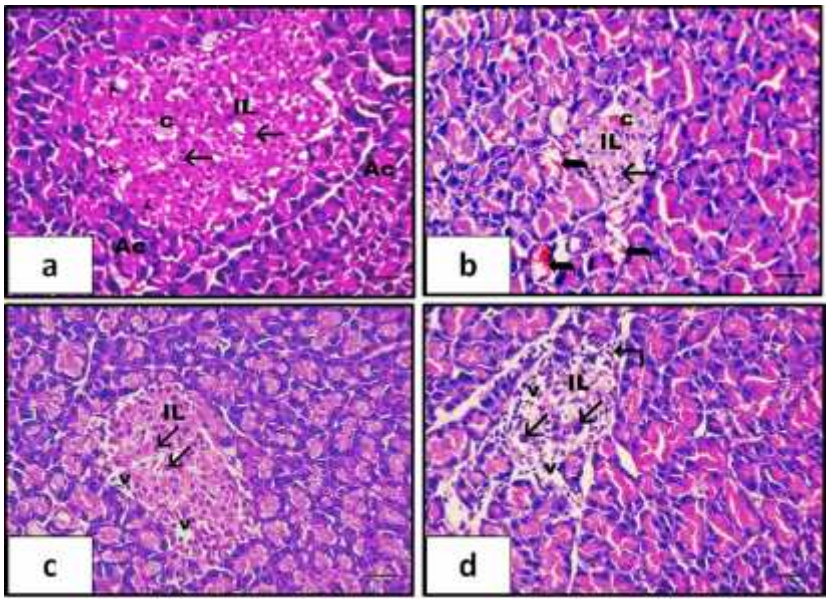


**Fig. 4**Photomicrograph from pancreas of experimental rats. (a) Normal control rat (G1), the pancreatic tissues of appeared to be normal. (b) Diabetic rats (G2) induced by HFD with STZ. The Higher magnification of the black-boxedareashowing islet of Langerhans thatappeared shrunken with irregular outlines. The islet cells apparently decreased in number with pyknotic nuclei (arrows) and congested capillaries in between (c). There were multiple congested blood vessels (bent arrows) between the exocrine acini. (c) Diabetic rats treated with resveratrol (RSV) (G3). Higher magnification of the black-boxed area showing nearly normal well defined islet of Langerhans (IL). The islet showed β-cells located in the center with vesicular nucleus (arrow), some cells still showing vacuolated cytoplasm (v). (d) Diabetic rat exposed to both RSV and chloroquine (CQ) (G4). Higher magnification of the black-boxed area showed distorted islet of Langerhans with irregular outlines. Some apoptotic cells (arrows) appeared with dense cytoplasm and pkknotic nuclei. Some other cells showed vacuolations (v). The CT septa infiltrated with inflammatory cells (angled arrow). (H&E, ×400) (Scale bar represents 25 µm).

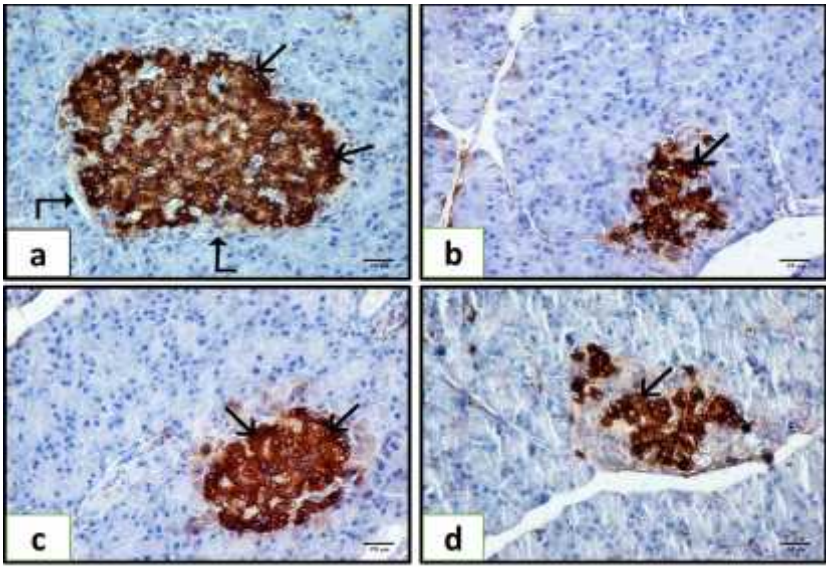


**Fig. 5**Insulin immunohistochemical staining sections of pancreatic isletsof experimental rats. (a) Normal control rat (G1), showing typical islet strong positive immunoreactivity of insulin appeared as deep brown color (arrow) in β-cells which occupy most of the islet and surrounded by pale mantle zone with negatively stained cells (angled arrow). (b) Diabetic rats (G2) induced by HFD with STZ and (d) Diabetic rat exposed to both RSV and chloroquine (CQ) (G4). They showing apparent marked reduction in the immunoreactivityof insulin in β-cells, only few cells showing brown immunostaining (arrow). (c) Diabetic rats treated with resveratrol (RSV) (G3) showing an apparent increase in the immunoreactivity of insulin β-cells (arrow) mostly similar to the controlgroup. (Anti-insulin, ×400) (Scale barrepresents 25µm).

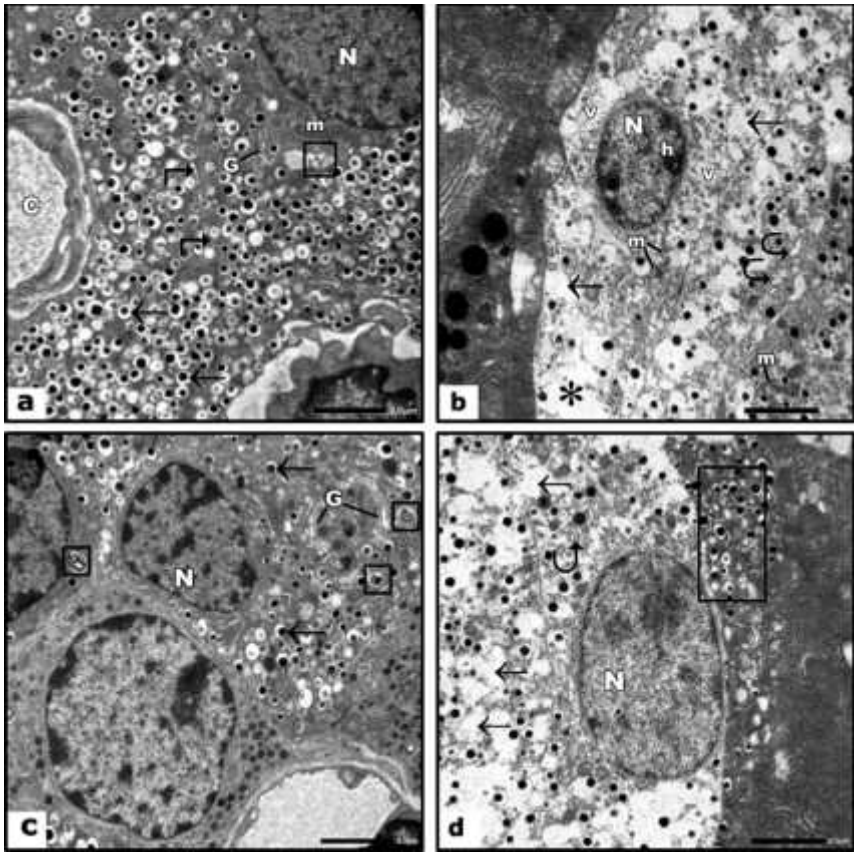


**Fig. 6** Transmission electron micrograph of the pancreatic tissue of experimental rats.(a) Normal control rat (G1), showing normal architecture of the β-cell with euchromatic nucleus (N), well-developed Golgi complex (G), mitochondria (m), an electron-dense insulin granules surrounded by lucent halos (arrow) and an autophagosome (square). The cell junctions (angled arrow) between β-cells and blood capillary in the islet (C) can be seen. (b) Diabetic rats (G2) induced by HFD with STZ, showingdegenerated β-cell with nuclear shrinkage (N), electron dense heterochromatin (h), cytoplasmic rarefaction with marked vacuolation (v), degenerated mitochondria (m), empty insulin granules (arrows) and cystic dilatation of the rough endoplasmic reticulum (curved-arrow). There were large areas of lost granules (a strike). (d) Diabetic rat exposed to both RSV and chloroquine (CQ) (G4), showing degenerated β-cell with empty insulin granules (arrows) and cystic dilatation rER (curved-arrow). The adjacent β-cell showed nearly normal insulin granules (rectangle). (c) Diabetic ratstreated with resveratrol (RSV) (G3), showingnearly normal β-cell except for slight chromatin condensation in the nucleus (N). The cytoplasm showed nearly normal insulin granules (arrows) and some autophagosomes (squares). (TEM),(Scale bar represents 2 µm).

## Discussion

This study was designed to investigate the effectiveness of RSV in maintaining pancreatic functioning in Wistar rats given HFD and STZ to induce T2DM. Deficiencies in insulin synthesis by pancreatic β-cells or its effect in peripheral tissues characterize diabetes mellitus, a chronic endocrine condition. Patients with T2DM have decreased cell mass and function in their β-cells in pancreatic islets, which is due to increased cell death;Consequently, preventing β-cell death is a possible key therapeutic approach [26].In the current study, rats receiving HFD plus STZ did not exhibit any overt clinical indicators of harmfulness and no evidence of stress were observed in the rats.

This study showed that in the diabetic group (G2), which suggests diabetes mellitus, fasting serum glucose levels dramatically increased while serum insulin levels noticeably fell. The elevated level of serum glucose and decrease level of insulin may have been due to young rats (4-5 weeks old) that received HFD with STZ presenting depletion of β-cell mass;the use of HFD is efficient for the

induction of T2DM, as the amount of lipids used in the diet in the present study was 30.03 % compared to the balanced diet (5.08 %). Also, STZ is a chemical that promotes damage to pancreatic β-cells and decrease insulin production[27]. The glucose transport protein moves STZ into β-cells of the pancreatic islets, but the other glucose carriers do not detect it. Since the pancreatic islets have relatively high quantities of the glucose transporter 2GLUT2, this negates its overall risk to the β-cells[28]. In a prior studyVatandoust et al[27], a comparable rise in blood sugar and fall in insulin levels brought on by HFD-STZ were noted.A glucosamine-nitrosourea molecule as STZ is bad for cells because it damages DNA. Poly ADP-ribosylation is initiated by DNA damage, and it is likely more important for the development of diabetes than DNA damage itself. Because β-cells of the pancreas are more susceptible than other cells to the STZ challenge, STZ reduces nicotinamide-adenine dinucleotide (NAD) in these cells, which leads to -cell degeneration in the islet of Langerhans and intermediates the induction of diabetes within three days [28].

When diabetic rats were treated with RSV, a significant rise in insulin levels and a decline in blood glucose levels were seen. This result may have been brought about by RSV's protective qualities. It improves preservation of pancreatic β-cells, due to its anti-diabetic, anti-inflammatory, and antioxidative properties [29]. According to a previous studyDarwish et al[29] RSV was prepared to lessen the damage STZ caused to pancreaticβ-cells.On the other hand, diabetic rats treated with both RSV and CQ show a considerable rise in serum glucose and a significant fall in insulin levels. This outcome might have been due to the inhibitory effects of CQ. It is believed that CQ increases the pH of lysosomes, which inhibits lysosomal action in pancreatic β-cells [30].

In the current study, lipid profile analysis showed a marked increase in the TG, TC, and LDL-C with significant decrease in HDL-C in the diabetic group after 10 weeks of receiving HFD-STZ that indicates dyslipidemia. Alteration of the lipid profile is commonly associated with HFD-STZ induced T2DM. Long-term HFD feeding (10 weeks) is linked to the release of fatty acids into the bloodstream, causing secondary triglyceridemia, where the levels of TG, TC, and LDL are elevated while HDL-C is decreased. This will consequently lead to aberrant blood lipid profiles, which cause life-threatening [31]. These changes enhanced cholesterol biosynthesis resulting from HFD. The increased levels of LDL-C may have resulted from the LDL-receptor sites' decreased activity in response to the HFD[31]. The most significant modifiable risk factor for T2DM atherosclerosis development is dyslipidemia; there is strong data point to a connection between coronary heart disease risk and high levels of circulating total cholesterol and low levels of HDL-C [32]. These results coincided with Ji et al[33] who fed rats HFD with the same dose of STZ (35 mg/kg b.wt.). The level of TG, TC, and LDL-Cwere markedly decreased, while there were no significant differences in the level of HDL-C when diabetic rats treated with RSV.RSV was discovered to have considerable anti-obesity effects by drastically suppressing increases in plasma lipid content. The proportion of LDL was where the majority of the decrease in plasma cholesterol occurred;this adjustment could be

attributable to a decrease in LDL-C, which improved the hypercholesterolemia brought on by HFD[34]. These results aligned with those from Zhu et al[34].

After 10 weeks of receiving HFD-STZ, the current study found that the diabetic group's MDA value significantly increased while the GSH and SOD values significantly fell, indicating oxidative stress.It is widely known that hyperglycemia increases the generation of reactive oxygen species (ROS) in the mitochondria, which may be a crucial step in the onset and progression of diabetic problems[35]. Superoxide anion production as ROS causes apoptotic cell death in a timely manner, nonenzymatic glycation of proteins, and glucose autoxidation;in addition, enhanced mitochondrial uncoupling and β-oxidation brought on by high levels of free fatty acids may potentially contribute to the increased production of ROS [36].On the other hand, when diabetic rats were treated with RSV, there was a significant rise in the level of GSH and SOD and a considerable drop in the amount of MDA. These results are consistent with those ofHamadi et al[36],who noted the antioxidant benefits of RSV in diabetic liver injury. RSV possesses antioxidant potential.

Confirming these findings,the histological images of the pancreas of RSV-treated rats showed an improvement when compared with the pancreas of diabetic rats (G2) that showedill-defined areas of endocrine pancreas with marked histological distortion. The islet of Langerhansappeared shrunken with irregular outlines, decreased in number with pyknotic nuclei and congested capillaries in between. These results matched those of an earlier study Abdel-Bakky et al[37]. Also diabetic rats treated with both RSV and CQ showed marked histological alterations in the structure of endocrine pancreas, distorted islet of Langerhans with irregular outlines, and some apoptotic cells appeared with dense cytoplasm and pyknotic nuclei. Some other cells showed vacuolations. The CT septa infiltrated with inflammatory cells. These findings confirmed that CQ have inhibitory effect on diabetic rats treated with RSV. While diabetic rats treated with RSV (G3) resulted in the nearly normal appearance of the pancreas. It showed well defined islet of Langerhans. The islet showed β-cells located in the center with vesicular nucleus, some cells still showing vacuolated cytoplasm. These results corroborated those of Darwish et al[29] who published related research.

On the other side, insulin immunohistochemicalstudy of pancreaticislets showed that diabetic rats exposed to both HFD with STZ and diabetic rats exposed to both RSV and CQ showed apparent marked reduction in the immunoreactivity of insulin in β-cells. While diabetic rats treated with RSV showed an apparent increase in the immunoreactivity of insulin β-cells as the control group. These findings coincided with Abdel-Bakky et al[37] who observed the increase in the immunoreactivity of insulin β-cells in diabetic rats treated with RSV.

We researched the functions of autophagy and apoptosis to better understand the involvement of RSV in diabetes. The maintenance of cell homeostasis is aided by the autophagy produced by numerous damaging stimuli.In order to protect organisms during times of increased cellular distress, autophagy primarily functions as an adaptive or "programmed cell survival" mechanism[25].The results of the current

investigation showed that after 10 weeks of the trial, the diabetic group had a significantly higher level of mTOR, Cas-3, and P62 and a significantly lower level of LC3 in pancreatic tissue, which indicates apoptotic-mediated cell death.Hyperglycemia associated hyperlipidemia induced ROS generation resulted in oxidative stress. These oxidative stress disturbed the levels of autophagy markers, indicated by significant decrease in the LC3, with significant increase in the p62 resulted in blocking the autophagic flux in pancreatic β-cells [30]. The significant increase in mTOR and Cas-3 indicating apoptotic activity with deficient autophagy process that referred to glucolipotoxicity under increased inflammatory and oxidative stress conditions due to nutrient overload[38]. The current research supports the findings of Fujitani et al[39]about autophagy and apoptosis in diabetes and its complications.

In contrast, following 10 weeks of the trial, treatment with RSV in the diabetic group revealed significantly lower levels of mTOR, Cas-3, and p62 protein markers in pancreatic tissue and significantly higher levels of LC3 compared to the diabetic group. These findings attributed to anti-apoptotic effects of RSV on pancreatic β-cells via inhibiting the mTOR pathway [40]. Treatment with RSV activated autophagy and inhibited the rate of apoptosis in β-cells, as evidenced by the significant increase level of LC3 and significant decrease p62 level.Additionally, RSV therapy significantly reduced the level of mTOR, indicating that it protected pancreatic β-cells by reversing the activation of mTOR caused by glucolipotoxicity. These findings agree withBostancıeri et al[40]Who explained the role of RSV in restored the levels of autophagy machinery andautophagic flux in diabetic cardiac cells through activation AMPK, and suppressing mTOR.

On the other side, the use of CQ (as autophagy inhibitor) in the diabetic group treated with both RSV and CQ, verify the relationship between autophagy-activation and the anti-apoptotic effect of RSV and to confirm autophagy's participation in mediating RSV's protective effects on diabetes.Lysosome accumulation and autophagy blocking are the results of CQ's ability to prevent lysosomal acidification, which reverses autophagy [30]. Additionally, CQ blocks the last stage of both the conventional and unconventional autophagy processes by inhibitingautophagosome-lysosome fusion [30].

Transmission electron micrograph (TEM) is the sole method capable of demonstrating the actual presence of subcellular autophagic structures such autophagosomes, lysosomes, and autophagolysosomes, making it the gold standard for autophagy monitoring[41]. The present study revealed that, Diabetic rats exposed to HFD and STZ showed degenerated β-cells with nuclear shrinkage, electron dense heterochromatin, cytoplasmic rarefaction with marked vacuolation, degenerated mitochondria, empty insulin granules, and cystic dilatation of the rough endoplasmic reticulum. There were large areas of lost granules. These findings indicates apoptotic cell death and autophagy inhibition [29]. On the other side, diabetic rats treated with RSV showed nearly normal β-cell except for slight chromatin condensation in the nucleus. The cytoplasm showed normal insulin granules and some autophagosomes.These findings indicates autophagy activation [37]. The diabetic rats treated

with both RSV and CQ showed degenerated β-cell with empty insulin granules and cystic dilatation rER; indicates autophagy inhibitory effects of CQ [30]. TEM of the pancreatic tissue on the control rats showed normal architecture of the β-cell with euchromatic nucleus. These results support the assertion made by Darwish et al[29] that RSV is effective in defending pancreatic tissues.

**Conclusions**

The current work showed that, in response to diabetes stimulation, RSV protects pancreatic β-cells by controlling the transition between autophagy and apoptotic machinery.The results suggest that RSV reduces ROS production that suppressed glucolipotoxicity induced apoptosis via autophagy activation through inhibition of mTORpathway. Therefore, autophagy is required to preserve the pancreatic β-cells' bulk, structure, and functionality.

**Consent to participate**

Acceptance of participation,each individual participant in this study provided both oral and written informed permission.

**Consent for publication**

All authors give their consent to publish this article in Bulletin of Egyptian society for physiological sciences.

**Author contribution**

L.A.M., N.O.E., H.E.N., and H.B.: designed the study, collected the samples and formal analysis.A.M.H.: analyzed the data and wrote the manuscript.W.B.E., S.A.E., and H.A.E.:original draft preparation. All authors read and approved the final manuscript.

**Acknowledgment**

The authors are grateful to Professor Dr. Nasser El-Sayed Khedr, Professor of Clinical Nutrition, Faculty of Veterinary Medicine, Benha University, Egypt, for his valuable support.

**Funding information**

None.

**Conflict of interest**

The authors declare no competing interests.

**Data availability**

The corresponding author will deliver the information needed to back up this study's conclusions upon request.

**References**

1. **He Q, Xu J-Y, Gu J, Tong X, Wan Z, Gu Y, et al.** Piperine is capable of improving pancreatic β-cell apoptosis in high fat diet and streptozotocin induced diabetic mice. Journal of Functional Foods 88:104890,2022.
2. **Rabanal-Ruiz Y, Korolchuk VI.** The role of lysosomes in autophagy. Autophagy in Health and Disease: Elsevier 2022: 57-70, 2022.
3. **Kreher C, Favret J, Maulik M, Shin D.** Lysosomal functions in glia associated with neurodegeneration. Biomolecules 11(3):400, 2021.
4. **Mir SU, George NM, Zahoor L, Harms R, Guinn Z, Sarvetnick NE.** Inhibition of autophagic turnover in β-cells by fatty acids and glucose leads to apoptotic cell death. Journal of biological chemistry 290(10):6071-6085, 2015
5. **Lytrivi M, Castell A-L, Poitout V, Cnop M.** Recent insights into mechanisms of β-cell lipo- and glucolipotoxicity in type 2 diabetes. Journal of molecular biology 432(5):1514-1534, 2020.
6. **Li H, Zheng F, Zhang Y, Sun J, Gao F, Shi G.** Resveratrol, novel application by preconditioning to attenuate myocardial

ischemia/reperfusion injury in mice through regulate AMPK pathway and autophagy level. Journal of Cellular and Molecular Medicine 26(15):4216-4229, 2022.

7. **Zhang J, Ping J, Jiang N, Xu L.** Resveratrol inhibits hepatic stellate cell activation by regulating autophagy and apoptosis through the SIRT1 and JNK signaling pathways. 2022.
8. **Abdelfadeel KF, Abdel Hamid OI, Alazouny ZM.** Resveratrol Ameliorates Hydroxychloroquine-Induced Retinopathy by Autophagy Induction: Molecular and Morphological Evidences. Zagazig University Medical Journal. 2022.
9. **Council NR.** Nutrient requirements of laboratory animals: 1995, 1995.
10. **Sihota P, Yadav RN, Poleboina S, Mehandia V, Bhadada SK, Tikoo K, et al**. Development of HFD-Fed/Low-Dose STZ-Treated Female Sprague-Dawley Rat Model to Investigate Diabetic Bone Fragility at Different Organization Levels. JBMR plus. 4(10): 10379, 2020.
11. **Kapucu, Ayşegül.**Crocin ameliorates oxidative stress and suppresses renal damage in streptozotocin induced diabetic male rats. Biotechnic & Histochemistry. 96(2):153-160, 2021.
12. **Mohammed F, Gurigis A, Abdel-Mageed W, Nassr A.** Improvement of insulin sensitivity and maintenance of glucose homeostasis in insulin-sensitive tissues via PPAR-γ and through activation of PI3K/p-Akt signaling pathway by resveratrol in type 2 diabetic rats. J Mol Immunol 3(119):2, 2018.
13. **Song S, Tan J, Miao Y, Sun Z, Zhang Q.** Intermittent-hypoxia-induced autophagy activation through the ER-stress-related PERK/eIF2α/ATF4 pathway is a protective response to pancreatic β-cell apoptosis. Cellular Physiology and Biochemistry 51(6):2955-2971, 2018.
14. **El-Shaer NO, Hegazy AM, Muhammad MH.** Protective effect of quercetin on pulmonary dysfunction in streptozotocin-induced diabetic rats via inhibition of NLRP3 signaling pathway. Environmental Science and Pollution Research 30:42390–42398, 2023.
15. **Trinder P.** Determination of glucose in blood using glucose oxidase with an alternative oxygen acceptor. Annals of clinical Biochemistry 6(1):24-27, 1969.
16. **Groen J, Kamminga C, Willebrands A, Blickman J.** Evidence for the presence of insulin in blood serum. A method for an approximate determination of the insulin content of blood. The Journal of Clinical Investigation 31(1):97-106, 1952.
17. **Cox RA, García-Palmieri MR.** Cholesterol, triglycerides, and associated lipoproteins 2011.
18. **Martin SS, Blaha MJ, Elshazly MB, Brinton EA, Toth PP, McEvoy JW, et al.** Friedewald-estimated versus directly measured low-density lipoprotein cholesterol and treatment implications. Journal of the American College of Cardiology 62(8):732-739, 2013.
19. **Garcia YJ, Rodríguez-Malaver AJ, Peñaloza N.** Lipid peroxidation measurement by thiobarbituric acid assay in rat cerebellar slices. Journal of neuroscience methods 144(1):127-135, 2005.
20. **Flohe L.** Superoxide dismutase assays. Methods in enzymology. 105: Elsevier 93-104, 1984.

**21. Ellman GL.** Tissue sulfhydryl groups. Archives of biochemistry and biophysics 82(1):70-77, 1959.

**22. Lowry OH.** Protein measurement with the Folin phenol reagent. J biol Chem 193:265-275, 1951.

**23. Suvarna KS, Layton C, Bancroft JD.** Bancroft's theory and practice of histological techniques E-Book: Elsevier health sciences; 2018.

**24. Campbell SC, Macfarlane WM.** Detection of insulin production by immunohistochemistry. Diabetes Mellitus: Springer:47-49, 2003.

**25. Ebrahim N, Ahmed IA, Hussien NI, Dessouky AA, Farid AS, Elshazly AM, et al.** Mesenchymal stem cell-derived exosomes ameliorated diabetic nephropathy by autophagy induction through the mTOR signaling pathway. Cells 7(12):226, 2018.

**26. Yong J, Johnson JD, Arvan P, Han J, Kaufman RJ.** Therapeutic opportunities for pancreatic β-cell ER stress in diabetes mellitus. Nature Reviews Endocrinology 17(8):455-467, 2021.

**27. Vatandoust N, Rami F, Salehi AR, Khosravi S, Dashti G, Eslami G, et al.** Novel high-fat diet formulation and streptozotocin treatment for induction of prediabetes and type 2 diabetes in rats. Advanced biomedical research 7, 2018.

**28. Tékus V, Horváth ÁI, Szabadfi K, Kovács-Valasek A, Dányádi B, Deres L, et al.** Protective effects of the novel amine-oxidase inhibitor multi-target drug SZV 1287 on streptozotocin-induced beta cell damage and diabetic complications in rats. Biomedicine & Pharmacotherapy 134:111105, 2021.

**29. Darwish MA, Abdel-Bakky MS, Messiha BA, Abo-Saif AA, Abo-Youssef AM.** Resveratrol mitigates pancreatic TF activation and autophagy-mediated beta cell death via inhibition of CXCL16/ox-LDL pathway: A novel protective mechanism against type 1 diabetes mellitus in mice. European Journal of Pharmacology 901:174059, 2021.

**30. Kanamori H, Takemura G, Goto K, Tsujimoto A, Mikami A, Ogino A, et al.** Autophagic adaptations in diabetic cardiomyopathy differ between type 1 and type 2 diabetes. Autophagy 11(7):1146-60, 2015.

**31. Luo J, Yang H, Song B-L.** Mechanisms and regulation of cholesterol homeostasis. Nature reviews Molecular cell biology 21(4):225-45, 2020.

**32. Maranta F, Cianfanelli L, Cianflone D.** Glycaemic control and vascular complications in diabetes mellitus type 2. Diabetes: from Research to Clinical Practice 4: 129-152, 2021.

**33. Ji J, Zhang C, Luo X, Wang L, Zhang R, Wang Z, et al.** Effect of stay-green wheat, a novel variety of wheat in China, on glucose and lipid metabolism in high-fat diet induced type 2 diabetic rats. Nutrients 7(7):5143-5155, 2015.

**34. Zhu K, Meng Z, Tian Y, Gu R, Xu Z, Fang H, et al.** Hypoglycemic and hypolipidemic effects of total glycosides of Cistanche tubulosa in diet/streptozotocin-induced diabetic rats. Journal of Ethnopharmacology 276:113991, 2021.

**35. Iacobini C, Vitale M, Pugliese G, Menini S.** Normalizing HIF-1α signaling improves cellular glucose metabolism and blocks the pathological pathways of hyperglycemic damage. Biomedicines 9(9):1139, 2021.

**36. Hamadi N, Mansour A, Hassan MH, Khalifi-Touhami F, Badary O.** Ameliorative effects of resveratrol on liver injury in streptozotocin-induced diabetic rats. Journal of biochemical and molecular toxicology 26(10):384-392, 2012.

**37. Abdel-Bakky MS, Alqasoumi A, Altowayan WM, Amin E, Darwish MA.** Resveratrol Inhibited ADAM10 Mediated CXCL16-Cleavage and T-Cells Recruitment to Pancreatic β-Cells in Type 1 Diabetes Mellitus in Mice. Pharmaceutics 14(3):594, 2022.

**38. Wang X-Y, Zhu B-R, Jia Q, Li Y-M, Wang T, Wang H-Y.** Cinnamtannin D1 protects pancreatic β-cells from glucolipotoxicity-induced apoptosis by enhancement of autophagy in vitro and in vivo. Journal of Agricultural and Food Chemistry 68(45):12617-12630, 2020.

**39. Fujitani Y, Kawamori R, Watada H.** The role of autophagy in pancreatic β-cell and diabetes. Autophagy 5(2):280-282, 2009.

**40. Bostancıeri N, Elbe H, Eşrefoğlu M, Vardı N.** Cardioprotective potential of melatonin, quercetin and resveratrol in an experimental model of diabetes. Biotechnic & Histochemistry 97(2):152-157, 2022.

**41. Liu W, Huang W, Ye L, Chen R, Yang C, Wu H, et al.** The activity and role of autophagy in the pathogenesis of diabetic nephropathy. Eur Rev Med Pharmacol Sci 22(10):3182-3189, 2018.